PNAS

An eosimiid primate of South Asian affinities in the Paleogene of Western Amazonia and the origin of New World monkeys

Laurent Marivaux[a,1] (ID), Francisco R. Negri[b], Pierre-Olivier Antoine[a] (ID), Narla S. Stutz[a,c] (ID), Fabien L. Condamine[a] (ID), Leonardo Kerber[d] (ID), François Pujos[e], Roberto Ventura Santos[f] (ID), André M. V. Alvim[f] (ID), Annie S. Hsiou[g] (ID), Marcos C. Bissaro Jr.[g], Karen Adami-Rodrigues[h] (ID), and Ana Maria Ribeiro[c,i] (ID)

Recent fossil discoveries in Western Amazonia revealed that two distinct anthropoid primate clades of African origin colonized South America near the Eocene/Oligocene transition (*ca.* 34 Ma). Here, we describe a diminutive fossil primate from Brazilian Amazonia and suggest that, surprisingly, a third clade of anthropoids was involved in the Paleogene colonization of South America by primates. This new taxon, *Ashaninkacebus simpsoni* gen. et sp. nov., has strong dental affinities with Asian African stem anthropoids: the Eosimiiformes. Morphology-based phylogenetic analyses of early Old World anthropoids and extinct and extant New World monkeys (platyrrhines) support relationships of both *Ashaninkacebus* and *Amamria* (late middle Eocene, North Africa) to the South Asian Eosimiidae. Afro-Arabia, then a mega island, played the role of a biogeographic stopover between South Asia and South America for anthropoid primates and hystricognathous rodents. The earliest primates from South America bear little adaptive resemblance to later Oligocene-early Miocene platyrrhine monkeys, and the scarcity of available paleontological data precludes elucidating firmly their affinities with or within Platyrrhini. Nonetheless, these data shed light on some of their life history traits, revealing a particularly small body size and a diet consisting primarily of insects and possibly fruit, which would have increased their chances of survival on a natural floating island during this extraordinary over-water trip to South America from Africa. Divergence-time estimates between Old and New World taxa indicate that the trans-atlantic dispersal(s) could source in the intense flooding events associated with the late middle Eocene climatic optimum (ca. 40.5 Ma) in Western Africa.

Brazilian Amazonia | Platyrrhini | teeth | phylogeny | paleobiogeography

Reconstructing the origins, historical biogeography, and early evolutionary histories of Neotropical platyrrhine primates and caviomorph rodents has long been among the most attractive and challenging issues in (paleo)mammalogy. These two groups are parts of those Asian African mammal clades (Anthropoidea and Hystricognathi, respectively), which appeared in the South American fossil record by mid-Cenozoic times. Thanks to a significant set of morphological and molecular evidence assembled over more than half a century, both groups are conjectured to have migrated across the South Atlantic Ocean from Africa to South America (1–10).

Recent paleontological efforts in the Paleogene of Western Amazonia, especially in the Andean foothills of Peru, have provided fundamental information on the early primates and rodents of South America (8, 11–20). In particular, they have shed light on their phylogenetic affinities with coeval late Eocene/early Oligocene African relatives and thus refined the timeframe for the colonization(s) of South America by both groups, which is consistent with estimates derived from molecular clock phylogenies (7, 9, 10, 21, 22). However, the pattern of colonization, notably for primates, turns out to be more complex than previously thought since the recent discoveries in Peruvian Amazonia [*Perupithecus* Bond et al. (12), and *Ucayalipithecus* Seiffert et al. (19)] reveal a polyphyletic colonization of South America by anthropoids of African origin. Along with the African hystricognath ancestor of caviomorph rodents, at least two basal anthropoid clades known in Africa (Oligopithecidae-like primates and Parapithecidae) colonized South America at the end of the Eocene epoch or near the Eocene/Oligocene transition (EOT), presumably via sweepstakes transatlantic dispersals (floating island rafting) (8, 12, 19). However, paleontological evidence remains scarce to comfort this biogeographic scenario.

Here, we report the discovery of a new fossil primate from Brazilian Amazonia (*Rio Juruá*, State of Acre). Although the taxon is documented by a single isolated tooth, it points to a third clade of basal anthropoids involved in the Paleogene colonization of South America by primates. This identification provides increasingly puzzling insights

Significance

Western Amazonia has recently revealed that two distinct anthropoid primate clades of African origin colonized South America near the Eocene/Oligocene transition (*ca.* 34 Ma). Here, we report a new fossil primate from Brazilian Amazonia pointing to a third clade involved in that colonization. Surprisingly, this taxon has strong affinities with eosimiid anthropoids of South Asian origin. These data highlight some of the life history traits (very-small-bodied size and insectivory/frugivory) that would have increased the chances of survival on a natural raft during this extraordinary transatlantic journey from Africa to South America. Estimated splits between New and Old World taxa indicate that the dispersal(s) coincides with the late middle Eocene climatic optimum (*ca.* 40.5 Ma), which generated intense flooding events.

into the origin and historical biogeography of New World monkeys, as the new taxon, *Ashaninkacebus simpsoni* gen et sp. nov., has strong affinities with stem anthropoid primates not of African but of South Asian origin: the Eosimiidae.

Results

Systematic Paleontology. Order Primates Linnaeus, 1758; Suborder Anthropoidea Mivart, 1864; Family Eosimiidae Beard, Qi, Dawson, Wang and Li, 1994.

Ashaninkacebus simpsoni gen. et sp. nov.

Etymology. The generic name refers to "*Asháninka*", a native ethnic group living in the rainforests of Western Amazonia, in Brazil (*Rio Juruá*, Acre), and more widely in Peru (*Río Alto Yurúa*, Ucayali, up to the watershed of the Peruvian Andes), with the Ancient Greek suffix κβος (*kêbos = cebus*), i.e., long-tailed monkey. Epithet in honor of the renowned evolutionary paleontologist George Gaylord Simpson, who co-led a joint Brazilian–American Museum paleontological expedition to the *Rio Juruá* in 1956. In recognition of the many fossil-bearing sites he discovered on this trip, but also for his courage after an accident he suffered on this river that almost cost him his life.

Holotype. UFAC-CS 066, right upper M1 (Fig. 1 *A–E*); the fossil is permanently housed in the collections of the Paleontology Laboratory of the Universidade Federal do Acre (UFAC), Floresta campus, Cruzeiro do Sul (CS), Acre, Brazil.

Type locality. *Ponto Rio Juruá* n°33' (PRJ-33'), situated on the left bank of the *Rio Juruá* (*Alto Yurúa*), 1 km upstream from the junction with the *Rio Breu* and the small village of *Foz do Breu*, Acre, Brazil (*SI Appendix*, Fig. S1).

Comments. The UFAC-CS 066 fossil specimen was recovered in allochthonous detrital Holocene sediments (PRJ-33', fine sand mixed with transported blocks of microconglomerate) deposited directly beneath the in situ PRJ-33 fossil-bearing locality, the latter being late middle Miocene in age, including the caviomorph rodents *Microscleromys* sp. (Chinchilloidea) and *Nuyuyomys* sp. (Erethizontoidea), both genera recognized in the Laventan South American Land Mammal Age at La Venta, Colombia, and TAR-31, Peru (23, 24). The precise upriver provenance and stratigraphic context of the UFAC-CS 066 primate tooth reported from PRJ-33' remain unknown. However, isolated teeth of caviomorph rodents documenting *Eoincamys* sp. [sp. 1] (25) as well as *Cachiyacuy* sp. [sp. 2] were found in the same PRJ-33' allochthonous primate-yielding sediments (*SI Appendix*, Fig. S2), thereby indicating a Paleogene age, likely around the EOT (i.e., *ca.* 34 Ma). These rodent genera are documented from several Peruvian fossil-bearing localities, notably from the geographically close Santa Rosa locality (*Alto Yurúa*, Ucayali [sp. 1+2]) (11, 18, 20), early Oligocene in age (26), from the Shapaja localities crossing the EOT (*Ríos Huallaga/Mayo*, San Martín [sp. 1]) (15, 27), and from some of the Contamana localities considered as preceding the EOT (*Quebrada Cachiyacu*, Loreto [sp. 2]) (8, 14, 28).

Age. Nearby the EOT (i.e., *ca.* 34 Ma), deriving from biochronological inferences. This temporal frame is independently corroborated by the median age estimate for *Ashaninkacebus* [≈32.9 Ma, 95% highest posterior density (HPD) = 42.1–19.9 Ma] deriving from a Bayesian tip-dating (BTD) analysis performed with a morphology-based phylogeny of basal anthropoid primates (+ extinct and extant Platyrrhini; see below Fig. 2).

Diagnosis (based on the holotype). Small-sized primate having upper molars low-crowned, transversely elongated, with a distal crown margin markedly invaginated, and primarily tritubercular with acute paracone, metacone and protocone, associated with a set of well-defined and sharp transverse and longitudinal crests (long and U-shaped pre- and postprotocone cristae, long hypoparacrista, short hypometacrista combined with a metacrista [= hypometacrista complex], and buccal shearing crests forming a long and complete eocrista); presence of a minute, not cuspate hypocone on a strong distolingual cingulum; buccal crown margin bearing a complete buccal cingulum, particularly expanded at the level of the metacone, and including a well-defined metastylar shelf; and no appreciable development of conules and parastyle (the dental terminology used here is presented in *SI Appendix*, Fig. S3).

Differential diagnosis (with Paleogene eosimiiform anthropoids). *Ashaninkacebus* differs from known Asian eosimiids, especially *Eosimias centennicus*, *Phenacopithecus krishtalkai* (middle Eocene, China), and *Bahinia banyueae* (early Oligocene, China) in being smaller, having a less angular and more smoothly rounded metastylar shelf, and in showing a quasi-non-development of the parastyle. It differs more specifically from *P. krishtalkai*, but also from *B. pondaungensis* (late middle Eocene, Myanmar) in being clearly smaller, displaying a lesser development of the mesial cingulum, lacking the entoprotocrista, and in having a buccal cingulum that is less developed and less extended buccomesially. Differs more particularly from *B. pondaungensis* in having a distal crown margin of the molar much more invaginated, displaying much less bulbous cusps, a lesser development of the hypometacrista complex,
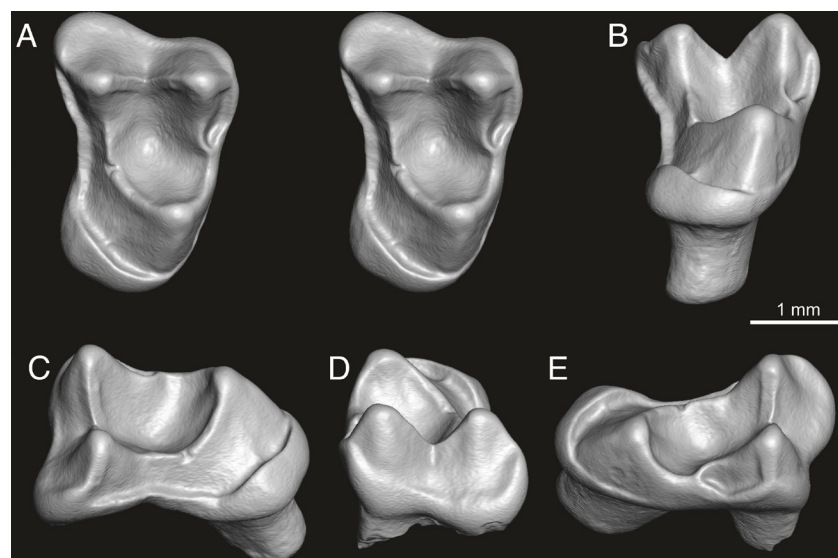
Fig. 1. Right first upper molar of *A. simpsoni* gen. et sp. nov. (UFAC-CS 066, holotype) from PRJ-33' locality, *Rio Juruá* (*Alto Yurúa*), State of Acre, Brazil. Buccolingual width: 2.92 mm; mesiodistal length: 2.03 mm. (*A*) Stereopair in occlusal view; (*B*) lingual view; (*C*) distal view; (*D*) buccal view; and (*E*) mesial view. Images are renderings of a 3D digital model of the fossil specimen, obtained by X-ray microcomputed (µCT) surface reconstruction (segmented enamel surface).

in lacking the development of an endoprotocrista in the trigon basin, and in showing a better development of the distolingual cingulum, which bears a minute hypocone. With the latter character condition, *Ashaninkacebus* also differs markedly from *B. banyueae* and *E. centennicus*. Differs from *Amamria tunisiensis* (late middle Eocene, Tunisia) in displaying a waisted rather than straight distal crown margin, in having a less pronounced shelf of the buccal cingulum, especially at the mesiobuccal corner of the crown, a more discrete mesial cingulum without pericone, stronger hypoparacrista and hypometacrista complex delimiting with the pre- and postprotocone cristae a more extensive trigon basin, and in displaying a cingular not cuspate hypocone. Differs from known Afro-Asian afrotarsiids (*Afrotarsius libycus* and *Afrasia djijidae*; late Eocene of Libya and late middle Eocene of Myanmar, respectively) in lacking the conules and, more especially, the postmetaconule crista (prominently developed on the M2 of *Afrasia* and *Afrotarsius*, but not on the M1 of *Afrasia*), in displaying a complete and continuous lingual cingulum with the development in the distolingual part of a minute hypocone (absent in afrotarsiids), and in having a more buccally extensive distal cingulum that reaches the base of the metastylar shelf, whereas it is limited near the midline of the crown in afrotarsiids (at least on the M2 of *Afrotarsius* and *Afrasia*, but not on the M1 of *Afrasia*). Differs more specifically from *Afrasia* in lacking the strong development of the parastyle in buccal position with respect to the paracone, and in showing a stronger development of the hypoparacrista and hypometacrista complex. *Ashaninkacebus* differs from *Phileosimias* (*P. kamali* and *P. brahuiorum*; early Oligocene, Pakistan) in lacking the conules, in having a stronger development of the lingual cingulum, a more invaginated distal margin, and in developing hypoparacrista and hypometacrista (both crests being absent in *Phileosimias*).

Description. A detailed description is provided in *SI Appendix, Text S1* (*SI Appendix,* Fig. S4).

Comparisons (with relevant simiiform anthropoids, including platyrrhines). *Ashaninkacebus* exhibits a suite of characters on the upper molar, which are primarily found in eosimiiform anthropoids. Some of these characters, such as the development of the buccal cingulum and the presence of a pronounced metastylar shelf (deriving from a buccal position of the metastyle with respect to the metacone and the presence of a long postmetacrista), are dental specializations of eosimiiforms, whereas some other characters, such as the deep invagination of the distal crown margin and the absence or weak development of a hypocone (cingular or cuspate hypocone but in the latter case remaining a very small tubercle), may be viewed as primitive (i.e., symplesiomorphies) compared to the dental patterns characterizing simiiform anthropoids. *Ashaninkacebus* appears somewhat as a morphological intermediate, at least based on the limited morphological information in the only available specimen, a single upper molar (M1). This intermediate status is suggested by the presence of a cingular hypocone (i.e., incipient development of a hypocone) and in the tendency to reduce the buccal cingulum and the metastylar shelf.

Ashaninkacebus differs from its South American companion, *Perupithecus ucayaliensis* (early Oligocene, Santa Rosa, Peru), in preserving the buccal cingulum and metastylar shelf (which are strongly reduced if not almost absent in *Perupithecus*, thereby placing its buccal cusps in a marginal position, with steep buccal flanks), in having a much higher degree of invagination of the distal crown margin, in lacking the entoprotocrista, and in displaying a weaker development of the hypoparacrista and hypometacrista complex. The M1 of *Ashaninkacebus* is also more transversely shaped, with a narrower trigon basin (i.e., narrow U-shaped pre- and postprotocone cristae, as in several other eosimiiforms). In contrast, in *Perupithecus*, as well as in North

African oligopithecids, proteopithecids, parapithecids and propliopithecids, some South Asian amphipithecids, and in stem and crown South American platyrrhines, upper molars are more quadrangular shaped, and their trigon basins are remarkably widened and vast in several cases (i.e., wider/flat U-shaped pre- and postprotocone cristae, with notably a more distally directed postprotocrista). On the other hand, the two unassigned tooth fragments (trigons of two upper molars; Collección Paleontológica del INGEMMET, Lima (CPI)-7000 and CPI-7001) found in association with *Perupithecus* in Santa Rosa (ref. 12, their figure 3 *C* and *D*) present interesting characteristics, being roughly similar both in size and morphology to the lingual region of the M1 of *Ashaninkacebus*. These lingual tooth fragments bear a small and limited-in-length mesial cingulum and a lingual cingulum that widens in its distal region (notably on CPI-7000, much less on CPI-7001), suggesting the presence of a cingular hypocone but much less pronounced than on UFAC-CS 066 of *Ashaninkacebus*. The distal region of CPI-7000 is better preserved than in CPI-7001 and reveals a somewhat deep invagination of the distal crown margin, close to that characterizing UFAC-CS 066. CPI-7000 preserves parts of the lingual flanks of the paracone and metacone, which display roughly similar development of the hypoparacrista and of the hypometacrista complex connected to the postprotocrista, as described on UFAC-CS 066. Although the buccal regions, highly diagnostic for *Ashaninkacebus*, are not preserved on these two specimens from Santa Rosa, based on the characters of their lingual parts, it is not excluded that the diminutive taxon represented by these two half-teeth is very closely related to *Ashaninkacebus*.

The oligopithecid *Oligopithecus rogeri* (early Oligocene, Oman) displays upper molars with a strong invagination of their distal crown margins, among the deepest observed in basal anthropoids, and does not show any development of a hypocone on the strong distolingual cingulum. In contrast, its closest relative, *Catopithecus browni* (latest Eocene, Egypt), has upper molars with a very weak invagination of their distal margins, as seen in *Perupithecus*, but unlike the latter, upper molars bear a small but well-defined and cuspate hypocone on their distolingual cingulum. The same applies to the proteopithecine parapithecid *Proteopithecus sylviae* (latest Eocene, Egypt), documented by upper molars with a more rectangular crown outline, without any distal invagination, and with the development of a distolingual hypocone. In most other basal simiiforms, including stem and crown platyrrhines (except callitrichine cebids), the quadrangular crown outline, without distal invagination, is mainly related to the development of the hypocone, which can become, in several cases, a full-fledged tubercle, as large as the three other main cusps.

Catopithecus and *Proteopithecus* display a moderately developed to discrete buccal cingulum on upper molars, whereas *Oligopithecus*, as *Perupithecus*, shows almost no development of the buccal cingulum or only a trace of it, a condition that is distinct from that of the eosimiiforms, and, in particular, *Ashaninkacebus*. Furthermore, in all these previous African taxa plus *Perupithecus*, there is no development of a prominent metastylar shelf as observed in eosimiiforms and *Ashaninkacebus*. A buccal cingulum may also be noticed in some Eocene and Oligocene African parapithecids (e.g., *Biretia, Apidium,* and *Simonsius*) and some South Asian amphipithecids (e.g., *Ganlea, Myanmarpithecus, Bugtipithecus,* and *Pondaungia*). However, this dental trait appears in these taxa most often as a trace, a vestige, or in most cases, it is limited between the two buccal cusps. It is never as buccally extensive as in eosimiiforms.

The development of a buccal cingulum is hardly ever observed in the upper molars of both basal and more advanced (crown)

platyrrhines of South America. At most, this cingulum occurs as a vestige in a very small number of basal taxa (*Parvimico* and *Mazzonicebus*; early Miocene, Peru and Argentina, respectively). In most platyrrhines (except several callitrichines), the buccal cusps are bulbous and their buccal flanks are generally steep-sided, without buccal cingulum (cusps positioned marginally). However, a few cases of buccal cingulum are observed in some large platyrrhine taxa (e.g., *Alouatta*, *Stirtonia*, and *Paralouatta*), seemingly secondarily acquired and linked to a specialized diet (folivory). Some modern platyrrhines (e.g., ateline atelids, and certain pitheciine pitheciids such as *Cacajao* and *Chiropotes*, or even the callicebine pitheciid *Xenothrix* from the Quaternary of Jamaica), in addition to lacking a buccal cingulum, also lack a lingual cingulum, despite the development of a strong hypocone. Most platyrrhines (except several callitrichines) are medium to large sized, and have quadritubercular upper molars with bulbous cusps. They also show a wide range of variations in the development (length and thickness) or nondevelopment of the buccal transverse crests (hypoparacrista and hypometacrista complex) and in the connection of the latter with the pre- and postprotocone cristae (the latter also showing a different degree of development). These dental conditions and variations correspond to specializations over time to specific diets (incidentally also associated with body-size changes); therefore, they are not directly comparable to the primitive dental pattern of small-bodied extinct species such as *Ashaninkacebus*, and even *Perupithecus*. Comparisons with small-bodied callitrichine cebids are certainly more relevant, although callitrichines also show dental specializations.

Callitrichines are somewhat peculiar among platyrrhines, not only by their small body size but also by their dental transformations/specializations, which led, among other things, to a strong reduction of the toothrow length and the loss in some taxa of the third molar (*Callithrix*, *Mico*, *Cebuella*, *Saguinus*, and *Leontopithecus*), associated with a reconfiguration of the second molar occlusal pattern and crown outline. Compared to the M1 of *Ashaninkacebus*, which is rather transversely arranged and distally waisted, callitrichines have a more triangular–quadrangular M1, with paracone and metacone slightly more distant from each other and with very little or no (*Cebuella* or the extinct *Lagonimico* from the late middle Miocene, Colombia) distal invagination of the crown. The lingual cingulum may be either strongly developed (*Lagonimico*, *Leontopithecus*, and *Callimico*), weakly developed (some species of *Callithrix*/*Mico*), or vestigial to absent (*Cebuella* and some species of *Callithrix*/*Mico*). When present, the lingual cingulum very rarely bears a hypocone in its distal region, as it does in *Ashaninkacebus* (cingular hypocone). Upper molars of some callitrichines (except in *Callimico*, *Leontopithecus*, and *Cebuella*) display a kind of buccal cingulum, which can be described as a mesio-distally extended enamel bulge (embedding the swollen bases of the paracone and metacone), rather than a full-fledged enamel shelf/fold. Unlike *Ashaninkacebus* and eosimiiforms in general, callitrichines have no metastyle or can display only a small enamel swelling, which is in line with the paracone–metacone axis. The postmetacrista is mostly absent or very weak, low and short when present, and there is no postmetacrista–metastylar shelf structure contrary to what is observed in *Ashaninkacebus* and eosimiiforms. In contrast, the distal cingulum can be much more buccally extensive than in eosimiiforms (or other basal anthropoids and several other platyrrhines), running at the base of the crown and surrounding the distobuccal aspect of the metacone. This condition is evident in several species of *Callithrix*/*Mico* and in *Cebuella* (as well as in *Parvimico*; early Miocene, Peru), in which the postmetacrista is very weakly developed or absent. A noticeable character of differentiation is the strong development of the hypoparacrista in *Ashaninkacebus*, whereas this crest is absent in callitrichines, and as such, the lingual flank of the

paracone is free-standing and steep sided in the latter. The absence or very weak development (very low and/or extremely short) vs. long and strong development of the hypoparacrista is variably distributed among platyrrhines. If this crest is particularly strong, long and trenchant in *Perupithecus*, in most stem platyrrhines (late Oligocene *Canaanimico* and *Branisella,* and early Miocene *Homunculus*, *Carlocebus*, *Soriacebus*, *Mazzonicebus*, and *Dolichocebus*) and in certain cebine and aotine cebids (*Panamacebus*, *Cebus*/*Sapajus*, *Acrecebus*, and *Aotus*), it is variably present in *Saimiri* and *Neosaimiri* (cebines), very weak to absent in extinct and extant pitheciids, and absent in extinct and extant atelids, in Quaternary West Indian *Antillothrix* and *Paralouatta*, and in *Parvimico*. As in *Ashaninkacebus*, the hypometacrista is also weakly developed and very short (or often absent) in callitrichines. Finally, as in *Ashaninkacebus*, callitrichines (and all other platyrrhines) display a well-developed distal metacrista, which may or may not be lingually connected to the postprotocrista. The latter is long and runs buccally in *Ashaninkacebus*, whereas it is variable in length and more distally directed in callitrichines (and platyrrhines in general).

Body mass (BM) estimates. Adult BM of *A. simpsoni* is estimated at 228 to 231 g on the basis of the M1 area (5.9276 mm^2), by using the two regression equations provided by Egi et al. (35) (*Materials and Methods*). This taxon was a diminutive primate with a BM much inferior to that estimated for the platyrrhine ancestral condition derived from comparative phylogenetic methods [i.e., ~400 g (36)]. *Ashaninkacebus* was about the size of some small living marmoset callitrichines [e.g., *Callithrix jacchus*, 236 to 256 g after Ford (37) or 317 to 324 g after Smith and Jungers (38); or *C. penicillata*, 182 to 225 g after Ford (37) or 307 to 344 g after Smith and Jungers (38)]; nonetheless, it was larger than the pygmy marmoset [*Cebuella pygmaea*, 126 to 130 g after Ford (37) or 110 to 122 g after Smith and Jungers (38)]. It was also likely of the same size as the extinct platyrrhine *Parvimico materdei* from lower Miocene deposits of Madre de Dios, Peru [235 to 239 g (39)], and slightly smaller than the South Asian eosimiid *E. centennicus* (~250 g) and afrotarsiid *A. djijidae* (~270 g) from the middle Eocene of China and Myanmar, respectively (30, 33). *Ashaninkacebus* was otherwise one-third smaller than *P. ucayaliensis* (477 to 494 g) from the early Oligocene Santa Rosa locality (Peru), the BM of which was more roughly close to that of some small living tamarin callitrichines [e.g., *Saguinus nigricollis*, 470 to 480 g after Ford (37) or 468 to 484 g after Smith and Jungers (38)]. *Ashaninkacebus* was also smaller bodied than *Ucayalipithecus perdita* from Santa Rosa, whose body size was estimated to be close to that of a medium-sized marmoset callitrichine [319 to 366 g (19)].

M1 shearing quotient (SQ) and diet reconstruction. Measurement of the M1 buccal cutting-edge development of *Ashaninkacebus* (*Materials and Methods*) reveals a positive and high SQ value (= 16.62), thereby reflecting well-developed shearing crests. Compared to platyrrhines with medium to small BMs (less than 1 kg; ref. 39, their figure 6*B*), the relatively high SQ and the very small body size of *Ashaninkacebus* indicate a diet with primarily insect and probably fruit consumption, but lacking exudates and leaves.

Phylogenetic analyses. We performed a cladistic assessment of the morphological evidence (A1 analysis) to investigate the phylogenetic position of *Ashaninkacebus* in a high-level phylogeny of basal anthropoids from the Old World (i.e., Paleogene South Asian and North African known taxa), plus known extinct and extant New World platyrrhines (*SI Appendix*, Table S1). The data matrix included 456 characters and 81 taxa (see *Materials and Methods* for character assumptions, data, and phylogenetic analyses; also, *SI Appendix*, Table S2 and *Text S2*). We enforced a
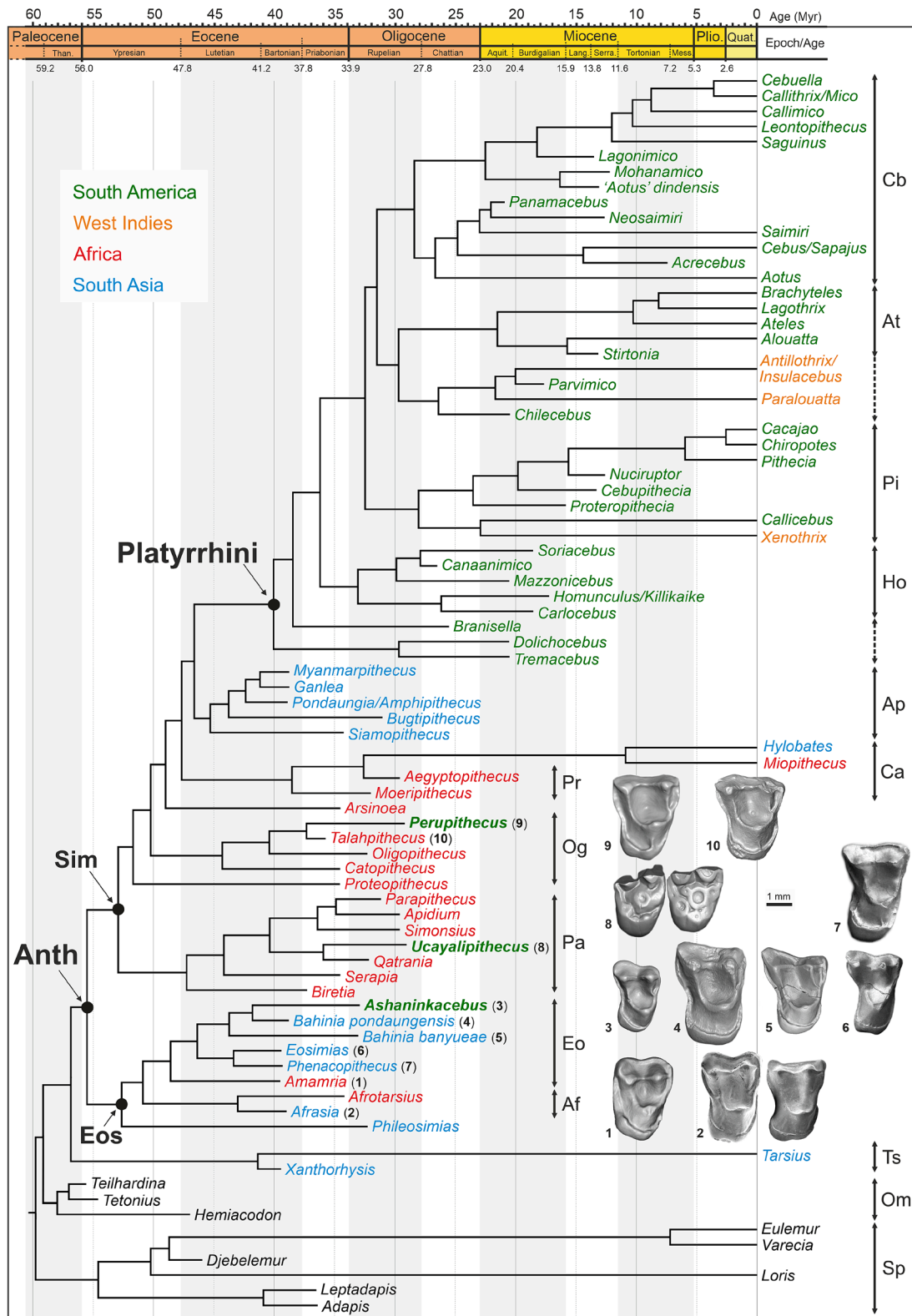
Fig. 2. Phylogenetic position of *A. simpsoni* gen. et sp. nov. in a high-level phylogeny of basal anthropoids (Old World, i.e., Paleogene South Asian and North African known taxa), plus known extinct and extant platyrrhines, deriving from a cladistic assessment of the craniodental and postcranial evidence. Single most parsimonious tree of 2,429.49 steps (consistency index [CI] = 0.36; retention index [RI] = 0.56), which was obtained after analyses performed in considering some ordered and scaled multistate characters, and in applying a molecular scaffold of living taxa relationships (*Materials and Methods*). The cladogram was then subjected to a Bayesian tip-dating analysis (BTD) for divergence-time estimation between taxa. Abbreviations: Af, Afrotarsiidae; Anth, Anthropoidea; Ap, Amphipithecidae; At, Atelidae; Ca, Catarrhini; Cb, Cebidae; Eo, Eosimiidae; Eos, Eosimiiformes; Ho, Homunculidae; Og, Oligopithecidae; Om, Omomyiformes; Pa, Parapithecidae; Pi, Pitheciidae; Pr, Propliopithecidae; Sim, Simiiformes; Sp, strepsirrhines; Ts, Tarsiidae. Upper molars of some basal anthropoids for comparisons: 1, KEB-1-001 right M2 of *Amamria tunisiensis* (ref. 29, their figure 3*A*); 2, NMMP-85 right M1 and NMMP-81 M2 of *Afrasia djijidae* (ref. 30, their figure 2 *A* and *B*); 3, UFAC-CS 066 right M1 of *A. simpsoni* gen. et sp. nov. (this paper); 4, M1 of the NMMP-15 right maxillary of *Bahinia pondaungensis* (ref. 31; here 3D rendering of a cast scan); 5, IVPP V22730 right M1 of *Bahinia banyueae* (ref. 32, their figure 1*F*); 6, IVPP V11993 left M1 (reversed) of *Eosimias centennicus* (ref. 33, their figure 9); 7, IVPP V11997 right M2 of *Phenacopithecus krishtalkai* (ref. 33, their figure 22), 8, CPI-7937 right M1 and CPI-7938 left M2 (reversed) of *Ucayalipithecus perdita* (ref. 19, their figure 1*A*); 9, CPI-6486 right M1 of *Perupithecus ucayaliensis* (refs. 12 and 19, their figure 1*D*); 10, DT1-31 left M1 (reversed) of *Talahpithecus parvus* (ref. 34, their figure 2*N*; here 3D rendering of a cast scan).

molecular backbone tree on the dataset to recover extant primate clades strongly supported by genomic sequences (*Materials and Methods*). The analyses yielded a single most parsimonious tree (2,429.49 steps, Consistency index = 0.36; Retention index = 0.56; Fig. 2 and *SI Appendix,* Fig. S5). These results show that the three oldest known primates from the early Oligocene of South America are not related to later platyrrhine monkeys but are nested within three distinct clades of Old World basal anthropoids (Fig. 2). *Ashaninkacebus* is nested within the Eosimiidae clade (sister to *Bahinia*), *Perupithecus* within the Oligopithecidae clade (sister to *Talahpithecus*), and *Ucayalipithecus* is nested within the Parapithecidae clade (sister to *Qatrania*) as formerly resolved by Seiffert et al. (19). Within Platyrrhini, we recover a pattern underscoring a stem radiation vs. crown radiation (40, 41), with, however, some changes regarding the Pleistocene Caribbean taxa (*Antillothrix/Insulacebus*, *Paralouatta*, and *Xenothrix*). The latter were previously resolved as stem platyrrhines (13, 41), but are interpreted here as crown platyrrhines. For the analysis, we have constrained the phylogenetic position of *Xenothrix* close to the Callicebinae, inasmuch as ancient DNA analyses recently demonstrated its pitheciid affinities (42). In contrast, *Paralouatta* and *Antillothrix/Insulacebus*, along with *Parvimico* and *Chilecebus*, are here resolved as a sister clade to the Atelidae, or stem Atelidae [as originally proposed for *Paralouatta* (43)], but see Kay et al. (39) for different results regarding these aforementioned taxa. These results may seem somewhat surprising in view of the phylogenetic position of the Paleogene South Asian Amphipithecidae, which branch quite high in the Anthropoidea clade, being resolved close to the Catarrhini clade, and as sister to Platyrrhini. However, this relationship is not strongly supported (Bremer support of 1; *SI Appendix,* Fig. S5), relying on a few morphological characters, possibly convergent (*SI Appendix, Text S3*). In this phylogenetic context, constraining the Amphipithecidae in a more basal position within the Anthropoidea clade [i.e., stem anthropoids, diverging after the Eosimiiformes (19, 44); A2 analysis] requires 12 additional steps (*SI Appendix,* Fig. S6).

The phylogenetic topology obtained by maximum parsimony (A1) was then subjected to a BTD analysis, for the sole purpose of estimating divergence times between taxa (*Materials and Methods* and *SI Appendix,* Table S2 and *Text S2*). All nodes of the age-free cladogram were applied as hard constraints for the BTD analysis (A3). We duplicated this BTD analysis in enforcing the topology considering the Amphipithecidae in a more basal position (A4). *Ashaninkacebus* was assigned to a broad age prior to these analyses since its stratigraphic context is unknown (*Materials and Methods*). The BTD analyses returned a median age of ≈32.9 Ma (95% HPD = 42.1 to 19.9 Ma) for this new taxon, an age that is consistent with the biochronological inferences derived from the caviomorph rodents found in association at PRJ-33' (i.e., nearby the EOT, *ca.* 34 Ma). Also of interest are the divergence-time estimates of the three ancient primates found in South America from their Old World counterparts, estimates which can be traced back to the late middle–late Eocene for *Perupithecus* (≈37.33 Ma, 95% HPD = 40.3 to 35.3 Ma), to the late middle Eocene–earliest Oligocene for *Ucayalipithecus* (≈35.93 Ma, 95% HPD = 40.6 to 32.0 Ma), and to the middle–late Eocene for *Ashaninkacebus* (≈41.8 Ma, 95% HPD = 45.5 to 38.9 Ma) (Fig. 2 and *SI Appendix,* Fig. S7 and Tables S3 and S4). It is worth mentioning the somewhat old age estimates derived from our BTD analysis (i.e., morphological clock analysis) regarding the emergence of the three main crown Platyrrhini families (Pitheciidae, Atelidae, and Cebidae), compared to molecular-based estimates (21, 22). Although older ages are expected under a BTD approach (45), our age estimates can be

inflated using morphological and/or morpho-paleontological data alone, without molecular data, since morphology does not evolve in the same "clock-like" manner as molecules (46, 47). Here, the crown platyrrhine radiation is traced back to the early Oligocene, resulting in a substantial incompleteness of the fossil record, while the stem platyrrhine radiation is estimated to extend back to the late middle Eocene (*SI Appendix,* Table S4). The latter estimates coincide to some extent with the divergence-time estimates of the three ancient South American primate fossils from their Old World counterparts, although no phylogenetic relationship can be formally established between *Ashaninkacebus* or *Perupithecus* and the stem platyrrhines yet (*Discussion*). Note that a basal placement of the Amphipithecidae clade (A4) has virtually no effect on the morphological clock analysis for estimating divergence times between taxa (*SI Appendix,* Fig. S8, Table S4, and *Text S3*).

Finally, we estimated simultaneously phylogenetic topology and divergence times of taxa in performing a partially constrained BTD analysis (A5), which enforced only the molecular backbone tree of living species and the topology of the branching groups of Anthropoidea plus outgroups as resolved in A1 (*Materials and Methods* and *SI Appendix,* Table S2). Despite some phylogenetic changes regarding a few taxa, this analysis did not result in conflicting topologies compared to the results of the parsimony analyses (*SI Appendix,* Fig. S9 and *Text S3*). The three oldest known primates from the early Oligocene of South America are also found here nested within the same three distinct clades of Old World basal anthropoids. *Ashaninkacebus* is resolved here as the earliest offshoot of the Eosimiidae clade among the Eosimiiformes. Its stemward phylogenetic position within the Eosimiidae affects the estimate of its median age, which is set back more than 6 My (≈38.8 Ma; 95% HPD = 45.0–25.8 Ma; *SI Appendix,* Table S4). Such an old age is otherwise inconsistent with the biochronological inferences assembled from PRJ-33'. Besides, the divergence-time estimate of *Ashaninkacebus* from other eosimiids is incredibly old (≈49.3 Ma; 95% HPD = 53.4–45.3 Ma; *SI Appendix,* Table S4) and somewhat unlikely (see our complementary discussion; *SI Appendix, Text S3*). From this BTD analysis (A5), the crown and stem platyrrhine radiations are estimated to have occurred slightly more recently than previously found in the A3 analysis (*SI Appendix,* Table S4), but still implying a substantial incompleteness of the platyrrhine fossil record. Outside of the Platyrrhini clade, this BTD analysis (A5) recovers the crownward branching of the Amphipithecidae within the Anthropoidea clade (*SI Appendix,* Fig. S9). Applying a stemward constraint on the branching of the Amphipithecidae (A6; *SI Appendix,* Fig. S10) did not impact the rest of the topology or the divergence-time estimates (*SI Appendix,* Table S4 and *Text S3*).

All these analyses (parsimony and the multiple BTD analyses) returned identical results regarding the eosimiid status of the new taxon *Ashaninkacebus*. Finally, we examined the uncertainty of the phylogenetic position of *Ashaninkacebus* across the posterior trees of the BTD analyses (A5 and A6), using the RoguePlots approach (48). In these two BTD analyses, *Ashaninkacebus* was always recovered nested within the Eosimiiformes (*SI Appendix,* Figs. S11 and S12).

Discussion

Macroevolutionary Implications. The oldest known primates from South America are so far represented only by a few isolated teeth, documenting three clearly distinct species: either much more primitive (*Perupithecus* and *Ashaninkacebus*) or radically different/specialized (*Ucayalipithecus*) with respect to any known platyrrhines. As a result, none of these earliest South American

anthropoid taxa is related to later platyrrhine monkeys (Fig. 2). *Perupithecus* was previously recovered at the root of Platyrrhini (19, 39, 47), but from phylogenetic analyses made with a much more restricted taxonomic sampling, i) excluding poorly known African Eocene taxa of utmost evolutionary interest, such as *Talahpithecus* and *Amamria*, and ii) lacking a comprehensive sampling of early-diverging anthropoids from the Paleogene of both Africa and Asia (39, 47). *Ucayalipithecus* is diverging and highly specialized compared to *Perupithecus*, *Ashaninkacebus,* and known basal platyrrhines. Its dental specialization (bulbous cusps, conules, styles, cuspids, and stylids, with limited crests and cristids; i.e., bunodonty) is similar to that of its coeval African parapithecid counterparts [i.e., primary frugivorous (19, 49)]. Such a specialization could have been selectively advantageous in the short term after the arrival of its lineage in South America, but ultimately resulted in low diversification, further leading to its extinction without leaving any extant relatives (i.e., evolutionary dead end). The very-small-bodied *Ashaninkacebus* and slightly larger *Perupithecus* have teeth much more crested (notably marked buccal shearing crests) and with acute cusps, indicating a mixed diet including primarily insects and also fruit [high SQ values; our results and those of Kay et al. (39)]. These two taxa are intriguing because they harbor dental patterns strikingly similar to those of some basal anthropoids such as South Asian eosimiids and African oligopithecids-like primates, respectively, but not to those of any known South American stem platyrrhines (late Oligocene and early Miocene in age). This raises the question of whether we should consider the dental patterns of *Ashaninkacebus* and *Perupithecus* to be highly convergent with those of these Old World basal anthropoids. From our assessment of the current dental evidence, they are interpreted as supporting phylogenetic affinities (Fig. 2). Insofar as the three oldest primates known to date in South America are nested in either African or South Asian clades, but not at the root of Platyrrhini, should we consider that we have not yet found a close relative of the platyrrhine ancestor? Should we also draw the conclusion of evolutionary dead ends for the lineages of *Ashaninkacebus* and *Perupithecus*? It is likely premature to answer these questions. Indeed, when analyzing evolutionary trends regarding upper molar character transformations over time within Anthropoidea or even in the closest outgroups of anthropoids (e.g., extinct tarsiiforms and adapiforms and extinct and extant strepsirrhines), the morphological changes from primitive dental structures characterizing *Ashaninkacebus* or *Perupithecus* toward derived structures observed in some early platyrrhines, such as *Dolichocebus, Homunculus, Carlocebus, Mazzonicebus, Canaanimico,* or *Parvimico*, are not structurally unrealistic (e.g., development of more bulbous cusps, increased size of the hypocone with a more quadrangular outline of the crown, and more developed crests in several cases). In other words, the dental patterns of *Ashaninkacebus* or *Perupithecus* could match the expected ancestral platyrrhine dental condition. That *Perupithecus* or *Ashaninkacebus* is the oldest known stem platyrrhine remains probable, but the limited morpho-paleontological data so far assembled (very few dental evidence and no cranial or postcranial data) do not allow formalizing either hypothesis. This means that rooting (technically) the Platyrrhini in an Old World anthropoid clade in which either *Ashaninkacebus* or *Perupithecus* is nested requires further morphological support than current data allow.

Paleobiogeographic Implications. In addition to the Parapithecidae (19) and Oligopithecidae-like primates (12) of African origin, the eosimiid affinities of *Ashaninkacebus* point to a third clade of basal anthropoids involved in the Paleogene colonization of South America by primates. Eosimiids are well documented in the Paleogene of South Asia (31–33, 50–52) but have not been formally recorded in the Eocene of Africa. However, our phylogenetic results resolved *Amamria* from the late middle Eocene of Tunisia [*ca.* 39.5 Ma (29)] nested within the Asian Eosimiidae clade (Fig. 2). *Amamria* is poorly documented (a single upper molar), but it represents, to date, the oldest known anthropoid primate in the fossil record of Africa. If it turns out that *Amamria* is indeed an eosimiid, this would support the hypothesis that this group of basal anthropoids of South Asian origin dispersed toward Africa, as was also the case for their closest relatives, the Afrotarsiidae (Fig. 2), and probably other basal anthropoids of Asian origin (29, 30, 34, 53). As surprising as it may seem, it is worth noting that while ancestral South Asian eosimiids dispersed across the Tethys Sea to invade Afro-Arabia sometime during the middle Eocene, they may also have continued their intercontinental dispersal across the Atlantic Ocean and colonized South America in the process. Afro-Arabia could have been a mega-island stopover (biogeographic crossroad) between South Asia and South America for anthropoid primates and hystricognathous rodents (8, 29, 54).

Given the polyphyletic pattern of early anthropoids observed in the Paleogene sparse fossil record of Western Amazonia, questions remain as to whether there was a single rafting event or several ones (simultaneous or staggered in time) from Africa to South America. The paleobiogeographic issue becomes even more complicated when considering also hystricognathous rodents ("mass transit" or iterative rafting events). Although the time window during which the Afro-South American dispersal(s) occurred is now better bracketed, how and which routes primates and rodents might have taken to reach South America is a matter of speculation. However, habitat preferences and certain paleobiological attributes specific to these basal anthropoid primates and hystricognathous rodents may have increased their chances of both being unwillingly embarked on natural rafts (i.e., pieces of land and plants detached from the margins of large rivers during intense flooding events) and surviving during such an extraordinary over-water trip to South America from Africa (and from South Asia to Africa; ref. 53). Small body sizes, insectivory/frugivory, arboreality (tree-dweller) in forested habitat near major river systems in Africa were likely key life-history traits that would have made these mammal groups especially prone to sweepstakes dispersal and survival on floating rafts, over larger-bodied, herbivorous animals living in forested or more open environments, away from riparian areas. Interestingly, our results of the BTD analysis suggest deep times for root age estimates, at least for the phylogenetic origins of *Ashaninkacebus* and *Perupithecus*, which can be traced back to the late middle Eocene (Fig. 2; an age range that is also estimated for the root of caviomorph rodents; refs. 16 and 26). The hyperthermal conditions of the late middle Eocene climatic optimum [MECO; ~40.5 Ma (55, 56)] resulted in particularly intense meteorological episodes in tropical/equatorial regions, most certainly associated with intense flooding events (e.g., refs. 57–59). These particular paleoenvironmental conditions may have enhanced riverbank break-ups more frequently, increasing the likelihood that some elements of riparian biological communities may have been carried away on natural rafts. Furthermore, the shorter distance between Africa and South America in the late middle Eocene might have increased the chances of successful transatlantic crossing(s) (6) rather than at a later time as advocated by Seiffert et al. (19), i.e., at or near the EOT, during which a major drop in sea level is recorded, but when the two landmasses were actually much further apart.

Trans-Tethyan dispersals of rodents and primates between South Asia and Africa (and/or other intervening landmasses) could also have been enhanced by the intense flooding events associated with the marked greenhouse climatic conditions of the MECO (29, 30, 34, 53, 54, 60).

The presence of these small-bodied anthropoid primates in lower Oligocene deposits of Western Amazonia demonstrates the resilience of these lineages to the constraints of such a transatlantic dispersal, and their remarkable capacity to adapt, especially in foraging behaviors, in these new environments that became accessible to them. *Ashaninkacebus* and *Perupithecus* reveal that the ecological niche of these oldest known anthropoid primates from South America differed significantly from that of subsequent platyrrhines (39, 61–63). Formalizing more precisely the potential phylogenetic links of these early South American primates with the first-known "true" platyrrhines would be a major achievement. This great challenge requires further paleontological data, especially substantial field efforts in tropical areas still severely under-sampled.

Materials and Methods

High-Resolution μCT Scan. The three-dimensional (3D) data presented in this work were produced through the technical facilities of the Instituto de Petróleo e dos Recursos Naturais, Pontifícia Universidade Católica do Rio Grande do Sul, Brazil (high-energy μCT-scanning station SkyScan 1173). The unique UFAC-CS 066 fossil tooth was scanned with a resolution of 5.64 μm. Avizo 2020.2 (Visualization Sciences Group) software was used for visualization, segmentation, and 3D rendering. The 3D digital model of the tooth is available on the online open-access platform MorphoMuseuM (64).

BM Estimation. Estimates of adult BM were obtained using regression equations provided by Egi et al. (35) based on the M1 area (maximum mesiodistal length times maximum buccolingual breadth). It was calculated from 1) all primate sample equation: $\ln BM = 1.713 \times \ln(M1\ area) - 4.535\ (RE = 1.012)$; and 2) the anthropoid equation: $\ln BM = 1.767 \times \ln(M1\ area) - 4.555\ (RE = 0.950)$. The ratio estimator (RE) is the correction for logarithmic transformation bias (39, 65). The correction is applied by multiplying the predicted BM by the RE.

Diet Reconstruction. An upper first molar SQ was calculated based on the sum of lengths of the buccal shearing crests 1 through 4 (66) with respect to the maximum mesiodistal tooth length (MDL). These lengths were measured on the 3D digital model of the UFAC-CS 066 M1 using Avizo 2020.2 measurement tools ("total shear" 1 to 4 = 2.84 mm; MDL = 2.03 mm). We followed the protocol of M1 SQ calculation and correction (using a Phylogenetic Generalized Least Squares model) provided and detailed in Kay et al. (39), modified from Allen et al. (67). We also used the platyrrhine dental measurement and diet dataset provided in Kay et al. (39).

Phylogenetic Reconstructions and Divergence-Time Estimation Between Taxa. The phylogenetic position of *Ashaninkacebus* in a high-level phylogeny including basal anthropoids (Old World, i.e., Paleogene South Asian and North African known taxa) and known extinct and extant platyrrhines was investigated (*SI Appendix*, Table S1). We performed a cladistic assessment of the dental evidence (plus cranial and postcranial characters for several other taxa), as well as BTD analyses on the same morphological dataset to estimate divergence times between taxa (and also both, i.e., phylogeny and divergence times). A summary of the different types of analyses performed (A1 to A6) is provided in *SI Appendix*, Table S2. We employed and updated the morphological matrix provided in Marivaux et al. (13), which itself was adapted and substantially modified from Kay (41). We incorporated in the matrix early anthropoid primates from the Paleogene of South Asia (i.e., Eosimiidae and Amphipithecidae) and North Africa (Parapithecidae, Oligopithecidae, and Propliopithecidae), as well as basal anthropoid taxa (*Amamria*, *Phileosimias*, *Afrasia*, and *Talahpithecus*), the phylogenetic status of some of which has not been formally established to date. The matrix also included primates recently identified in South America (basal anthropoids and early platyrrhines), although some are poorly documented

(*Perupithecus*, *Canaanimico*, *Panamacebus*, *Parvimico*, and *Ucayalipithecus*; *SI Appendix*, Table S1). All characters for all taxa in the total matrix were reexamined, and some upper and lower dentition characters were reinterpreted, adjusted, or added to better describe the extent and variation of character states within basal and advanced anthropoids and extinct and extant platyrrhines (Dataset S1). The final data matrix included 456 characters and 81 taxa (Datasets S2 and S3). We applied a molecular scaffold (68) on the datasets to recover those extant primate clades (Tarsiidae, Catarrhini, and Strepsirrhini) and notably Platyrrhini and within Platyrrhini clades that are strongly supported by genomic sequences. The gene-based tree of extant taxa used as a constraint derives from several consistent molecular phylogenetic results (e.g., refs. 21, 22, and 69). Among Platyrrhini, this backbone tree enforces the monophyly of the three main families (and subfamilies within): Cebidae (including Cebinae, Callitrichinae, and Aotinae), Atelidae (including Atelinae and Alouattinae), and Pitheciidae (including Callicebinae and Pitheciinae), the latter family being the most basal platyrrhine diverging clade. In our scaffold, Aotinae (*Aotus*) were considered as Cebidae *incertae sedis* since the competing hypotheses regarding their phylogenetic affinities either with cebines or callitrichines or even with both (70, 71). The Pleistocene Caribbean primate taxon *Xenothrix* was also constrained as closely related to the callicebine pitheciid *Callicebus/Cheracebus* following recent ancient DNA analyses (42).

Parsimony Analyses. For the cladistic analyses (A1 and A2; *SI Appendix*, Table S2), additive multistate characters (i.e., conforming to natural morphoclines) were considered as ordered and were scaled such that the sum of the steps equals 1 (13, 41). Characters were polarized via the outgroup comparison method (72) using extinct and extant strepsirrhine primates (adapiforms and stem and crown strepsirrhines) and branching haplorrhine groups (tarsiiforms). The matrix for the parsimony analyses is provided in Dataset S2. The phylogenetic reconstructions were performed with PAUP 4.0a 169 (73) by heuristic searches (Hsearch) using random step-wise addition (1,000 replications with randomized input order of taxa) and tree bisection–reconnection branch swapping options. Polymorphic vs. uncertain character states (multistate taxa) were considered, and both were treated distinctly by PAUP (option MSTaxa = Variable). The clade robustness was measured by the Bremer Index (74) in equally weighted maximum parsimony (after 1,000 iterations with randomized input order of taxa) (*SI Appendix*, Fig. S5).

BTD Analyses. This Bayesian approach considers both the ages of the fossil taxa (tips) and rates of character evolution (75). For all the BTD analyses performed (A3 to A6; *SI Appendix*, Table S2), we selected the conditional version of the 1-parameter Markov-*k* model (76) for our total dataset, which includes only morphological data. The independent gamma rate relaxed-clock model was applied to account for variation in morphological evolutionary rates among branches. The fossilized birth–death (FBD) process was used as a prior on branch lengths (in setting "samplestrat" to "fossiltip"), thus considering those tips left no descendant. Each fossil tip was calibrated with a uniform prior on age, corresponding to the minimum and maximum ages of each extinct taxon (i.e., stratigraphic range of a taxon, or upper and lower bounds of geological stages or Land Mammal Ages to which a fossil has been assigned, or even the error range of an absolute radiometric age; see *SI Appendix*, Table S1). Extant taxa were calibrated with a fixed prior on age set to present: fixed(0). Regarding *Ashaninkacebus*, its stratigraphic context being unknown (without considering the biochronological indication deriving from the associated rodent taxa from PRJ-33'), we have applied a very broad uniform temporal range prior on this taxon age, from the middle Eocene (45 Ma) to the late middle Miocene (13 Ma; the estimated age of the in situ PRJ-33 locality). The BTD analysis should return a median age estimate and a 95% HPD for *Ashaninkacebus* (e.g., ref. 77). The FBD process was informed with a prior on the speciation rate ("speciationpr") set to exp(50), and flat beta priors (1.0, 1.0) associated with the fossilization rate and relative extinction rate ("fossilizationpr" and "extinctionpr," respectively). The tree root age was constrained to fall within a uniform prior from 56 Ma to 60 Ma, beyond which no representative of Euprimates has been recognized in the fossil record. For the gamma distribution from which the branch lengths are drawn ("igrvarpr"), this prior was set to exp(3). The prior on the rate of morphological changes, measured in the number of changes per character per millions of years ("clockratepr"), was set to normal (0.25, 0.05). The BTD analyses were performed with MrBayes 3.2.7a (78), using the computer cluster CIPRES Science Gateway 3.3 (79). As for the parsimony analyses, additive multistate characters were considered as ordered. Unlike PAUP, MrBayes treats all cases of polymorphism and uncertainty in the matrix as missing data (i.e., "?"), a

drastic loss of morphological information that can seriously impact the phylogenetic reconstruction (*SI Appendix, Text S2*). Given this, we first performed a BTD analysis by applying as hard constraints all nodes of the cladogram obtained with PAUP (A1) to estimate only the divergence times among taxa, not the phylogenetic relationships via a Bayesian approach (A3; Fig. 2 and *SI Appendix*, Fig. S7 and *Text S3*). However, we also performed a partially constrained BTD analysis (A5) in enforcing only the molecular backbone tree of living species and the topology of the branching groups of Anthropoidea plus outgroups, as resolved in A1 (*SI Appendix*, Fig. S9 and *Text S3*). BTD analyses were also conducted considering the Amphipithecidae as stem Anthropoidea (A4 and A6; see *SI Appendix*, Table S2 and Figs. S8 and S10). The different topological constraints for MrBayes (A3 to A6) were generated with R 4.2.1 (80), using the "ape" (81) and "paleotree" (82) R packages. The matrix and command lines for the BTD analyses and their variants are provided in Datasets S3 and S4. For each BTD analysis, two independent runs were performed simultaneously with four Monte Carlo Markov Chains (MCMC), with one cold and three heated (temp = 0.01) for 50 million generations per run. The MCMC were sampled every 1,000 generations, with a burn-in percentage of 25%. Convergence was assessed by checking the effective sample size and the average SD of split frequencies in the final generation (*SI Appendix*, Table S3). For the A5 and A6 BTD analyses, an "allcompat" consensus tree was generated, summarizing all post-burn-in sampled trees. Several sensitivity analyses were performed with various perturbations of the priors, notably igrvarpr, clockratepr, and speciationpr (*SI Appendix, Text S4*), which returned similar age estimates. Finally, using the RoguePlots approach (48), we assessed the uncertainty of the phylogenetic position of *Ashaninkacebus* across the posterior trees of the BTD A5 and A6 analyses after excluding the burn-in period.

Data, Materials, and Software Availability. 3D model data have been deposited in MorphoMuseuM (10.18563/journal.m3.188) (64). All study data are included in the article and/or supporting information.

Author affiliations: ᵃLaboratoire de Paléontologie, Institut des Sciences de l'Évolution de Montpellier (UMR 5554, CNRS/Université de Montpellier/Institut de Recherche pour le Développement), Université de Montpellier, 34095 Montpellier, France; ᵇLaboratório de Paleontologia, Universidade Federal do Acre, 69980-000 Cruzeiro do Sul, Brazil; ᶜPrograma de Pós-Graduação em Geociências, Universidade Federal do Rio Grande do Sul, 91501-970 Porto Alegre, Brazil; ᵈCentro de Apoio à Pesquisa Paleontológica da Quarta Colônia, Universidade Federal de Santa Maria, 97230-000 São João do Polêsine, Brazil; ᵉInstituto Argentino de Nivología, Glaciología y Ciencias Ambientales, CONICET–Universidad Nacional de Cuyo-Mendoza, 5500 Mendoza, Argentina; ᶠLaboratório de Geocronologia, Instituto de Geociências, Universidade de Brasília, 70910-000 Brasília, Brazil; ᵍLaboratório de Paleontologia, Universidade de São Paulo, 14040-901 Ribeirão Preto, Brazil; ʰNúcleo de Estudos em Paleontologia e Estratigrafia, Centro das Engenharias, Universidade Federal de Pelotas, 96010-020 Pelotas, Brazil; and ᶦSeção de Paleontologia, Museu de Ciências Naturais, Secretaria do Meio Ambiente e Infraestrutura, 90690-000 Porto Alegre, Brazil

Author contributions: L.M., F.R.N., P.-O.A., and A.M.R. designed research; L.M., F.R.N., P.-O.A., N.S.S., L.K., F.P., R.V.S., A.M.V.A., A.S.H., M.C.B., K.A.-R., and A.M.R. performed research; F.L.C. contributed new reagents/analytic tools; L.M., N.S.S., F.L.C., and L.K. analyzed data; F.R.N. managed fieldwork seasons; P.-O.A., N.S.S., F.L.C., L.K., F.P., R.V.S., A.M.V.A., A.S.H., and A.M.R. reviewed the manuscript and provided edits; R.V.S. and A.M.V.A. analyzed the stratigraphical context; and L.M. wrote the paper.

1. R. Hoffstetter, R. Lavocat, Découverte dans le Déséadien de Bolivie de genres pentalophodontes appuyant les affinités des rongeurs caviomorphes. *C. R. Acad. Sci.* **271**, 172–175 (1970).
2. R. L. Ciochon, A. B. Chiarelli, "Paleobiogeographic perspectives on the origin of Platyrrhini" in *Evolutionary Biology of the New World Monkeys and Continental Drift*, R. L. Ciochon, A. B. Chiarelli, Eds. (Plenum Press, 1980), pp. 459–493.
3. A. Houle, The origin of platyrrhines: An evaluation of the Antarctic scenario and the floating island model. *Am. J. Phys. Anthropol.* **109**, 541–559 (1999).
4. J. G. Fleagle, C. C. Gilbert, "The biogeography of primate evolution: The role of plate tectonics, climate and chance" in *Primate Biogeography. Progress and Prospects*, S. M. Lehman, J. G. Fleagle, Eds. (Springer, 2006), pp. 375–418.
5. C. Poux, P. Chevret, D. Huchon, W. W. De Jong, E.J.-P. Douzery, Arrival and diversification of caviomorph rodents and platyrrhine primates in South America. *Syst. Biol.* **55**, 228–244 (2006).
6. F. Bandoni de Oliveira, E. C. Molina, G. Marroig, "Paleogeography of the South Atlantic: A route for primates and rodents into the New World?" in *South American Primates: Comparative Perspectives in the Study of Behavior, Ecology, and Conservation. Developments in Primatology. Progress and Prospects*, P. A. Garber, A. Estrada, J. C. Bicca-Marques, E. W. Heymann, K. B. Strier, Eds. (Springer+Business Media, 2009), pp. 55–68.
7. P. Perelman *et al.*, A molecular phylogeny of living primates. *PLoS Genetics* **7**, e1001342 (2011).
8. P.-O. Antoine *et al.*, Middle Eocene rodents from Peruvian Amazonia reveal the pattern and timing of caviomorph origins and biogeography. *Proc. Royal Soc. B* **279**, 1319–1326 (2012).
9. C. G. Schrago, A. N. Menezes, C. Furtado, C. R. Bonvicino, H. N. Seuànez, Multispecies coalescent analysis of the early diversification of Neotropical primates: Phylogenetic inference under strong gene trees/species tree conflict. *Gen. Biol. Evol.* **6**, 3105–3114 (2014).
10. N. S. Upham, B. D. Patterson, "Evolution of caviomorph rodents: A complete phylogeny and timetree for living genera" in *Biology of Caviomorph Rodents: Diversity and Evolution*, A. I. Vassallo, D. Antenucci, Eds. (SAREM Series A, 2015), pp. 63–120.
11. C. D. Frailey, K. E. Campbell, "Paleogene rodents from Amazonian Peru: The Santa Rosa local fauna" in *The Paleogene Mammalian Fauna of Santa Rosa, Amazonian Peru*, K. E. Campbell, Ed. (Natural History Museum of Los Angeles County, 2004), pp. 71–130.
12. M. Bond *et al.*, Eocene primates of South America and the African origins of New World monkeys. *Nature* **520**, 538–541 (2015).
13. L. Marivaux *et al.*, Neotropics provide insights into the emergence of New World monkeys: New dental evidence from the late Oligocene of Peruvian Amazonia. *J. Hum. Evol.* **97**, 159–175 (2016).
14. M. Boivin *et al.*, Late middle Eocene caviomorph rodents from Contamana, Peruvian Amazonia. *Palaeontol. Electron.* **50**, 1–50 (2017).
15. M. Boivin *et al.*, Early Oligocene caviomorph rodents from Shapaja, Peruvian Amazonia. *Palaeontographica Abt. A* **311**, 87–156 (2018).
16. M. Boivin, L. Marivaux, P.-O. Antoine, New insight from the Paleogene record of Amazonia into the early diversification of Caviomorpha (Hystricognathi, Rodentia): Phylogenetic, macroevolutionary and paleobiogeographic implications. *Geodiversitas* **41**, 143–245 (2019).
17. M. Boivin *et al.*, Eocene caviomorph rodents from Balsayacu (Peruvian Amazonia). *Paläontol. Zeitsch.* **96**, 135–160 (2022).
18. M. Arnal, A. G. Kramarz, M. G. Vucetich, C. D. Frailey, K. E. Campbell, New palaeogene caviomorphs (Rodentia, Hystricognathi) from Santa Rosa, Peru: Systematics, biochronology, biogeography and early evolutionary trends. *Pap. Palaeontol.* **6**, 193–216 (2020).
19. E. R. Seiffert *et al.*, A parapithecid stem anthropoid of African origin in the Paleogene of South America. *Science* **368**, 194–197 (2020).
20. M. Arnal, M. E. Pérez, L. M. Tejada Medina, K. E. Campbell, The high taxonomic diversity of the Palaeogene hystricognath rodents (Caviomorpha) from Santa Rosa (Peru, South America) framed within a new geochronological context. *Hist. Biol.* **34**, 2350–2373 (2022).
21. M. S. Springer *et al.*, Macroevolutionary dynamics and historical biogeography of primate diversification inferred from a species supermatrix. *PLoS One* **7**, e49547 (2012).
22. N. S. Upham, J. A. Esselstyn, W. Jetz, Inferring the mammal tree: Species-level sets of phylogenies for questions in ecology, evolution, and conservation. *PLoS Biol.* **17**, e3000494 (2019).
23. A. H. Walton, "24. Rodents" in *Vertebrate Paleontology in the Neotropics. The Miocene Fauna of La Venta, Colombia*, R. F. Kay, R. H. Madden, R. L. Cifelli, J. J. Flynn, Eds. (Smithsonian Institution Press, 1997), pp. 392–409.
24. M. Boivin *et al.*, Late middle Miocene caviomorph rodents from Tarapoto, Peruvian Amazonia. *PLoS One* **16**, e0258455 (2021).
25. L. Kerber *et al.*, Tropical fossil caviomorph rodents from the southwestern Brazilian Amazonia in the context of the South American faunas: Systematics, biochronology, and paleobiogeography. *J. Mammal. Evol.* **24**, 57–70 (2017).
26. K. E. Campbell Jr., P. B. O'Sullivan, J. G. Fleagle, D. De Vries, E. R. Seiffert, An early Oligocene age for the oldest known monkeys and rodents of South America. *Proc. Natl. Acad. Sci. U.S.A.* **118**, e2105956118 (2021).
27. P.-O. Antoine *et al.*, "Biotic community and landscape changes around the Eocene-Oligocene transition at Shapaja, Peruvian Amazonia: Regional or global drivers?" in *Exploring the Impact of Andean Uplift and Climate on Life Evolution and Landscape Modification: From Amazonia to Patagonia*, C. Hoorn, L. Palazzesi, D. Silvestro, Eds. (Global and Planetary Change, 2021), p. 103512.
28. P.-O. Antoine *et al.*, A 60-million-year Cenozoic history of western Amazonian ecosystems in Contamana, Eastern Peru. *Gondwana Res.* **31**, 30–59 (2016).

29. L. Marivaux *et al.*, A morphological intermediate between eosimiiform and simiiform primates from the late middle Eocene of Tunisia: Macroevolutionary and paleobiogeographic implications of early anthropoids. *Am. J. Phys. Anthropol.* **154**, 387–401 (2014).

30. Y. Chaimanee *et al.*, A new middle Eocene primate from Myanmar and the initial anthropoid colonization of Africa. *Proc. Natl. Acad. Sci. U.S.A.* **109**, 10293–10297 (2012).

31. J.-J. Jaeger *et al.*, A new primate from the middle Eocene of Myanmar and the Asian early origin of anthropoids. *Science* **286**, 528–530 (1999).

32. X. Ni, Q. Li, L. Li, K. C. Beard, Oligocene primates from China reveal divergence between African and Asian primate evolution. *Science* **352**, 673–677 (2016).

33. K. C. Beard, J. Wang, The eosimiid primates (Anthropoidea) of the heti formation, Yuanqu Basin, Shanxi and Henan Provinces, People's Republic of China. *J. Hum. Evol.* **46**, 401–432 (2004).

34. J.-J. Jaeger *et al.*, Late middle Eocene epoch of Libya yields earliest known radiation of African anthropoids. *Nature* **467**, 1095–1098 (2010).

35. N. Egi, M. Takai, N. Shigehara, T. Tsubamoto, Body mass estimates for Eocene eosimiid and amphipithecid primates using prosimian and anthropoid scaling models. *Int. J. Primatol.* **25**, 211–236 (2004).

36. D. Silvestro *et al.*, Early arrival and climatically-linked geographic expansion of New World Monkeys from tiny African ancestors. *Syst. Biol.* **68**, 78–92 (2018).

37. S. M. Ford, Evolution of sexual dimorphism in body weight in platyrrhines. *Am. J. Primatol.* **34**, 221–244 (1994).

38. R. J. Smith, W. L. Jungers, Body mass in comparative primatology. *J. Hum. Evol.* **32**, 523–559 (1997).

39. R. F. Kay *et al.*, *Parvimico materdei* gen. et sp. nov.: A new platyrrhine from the Early Miocene of the Amazon Basin, Peru. *J. Hum. Evol.* **134**, 102628 (2019).

40. R. F. Kay, J. G. Fleagle, Stem taxa, homoplasy, long lineages, and the phylogenetic position of *Dolichocebus*. *J. Hum. Evol.* **59**, 218–222 (2010).

41. R. F. Kay, Biogeography in deep time–What do phylogenetics, geology, and paleoclimate tell us about early platyrrhine evolution? *Mol. Phylogenet. Evol.* **82**, 358–374 (2015).

42. R. Woods, S. T. Turvey, S. Brace, R. D. E. MacPhee, I. Barnes, Ancient DNA of the extinct Jamaican monkey *Xenothrix* reveals extreme insular change within a morphologically conservative radiation. *Proc. Natl. Acad. Sci. U.S.A.* **115**, 12769–12774 (2018).

43. M. Rivero, O. Arredondo, *Paralouatta varonai*, a new quaternary platyrrhine from Cuba. *J. Hum. Evol.* **21**, 1–11 (1991).

44. J.-J. Jaeger *et al.*, Amphipithecine primates are stem anthropoids: Cranial and postcranial evidence. *Proc. Royal Soc. B* **287**, 20202129 (2020).

45. J. E. O'Reilly, M. Dos Reis, P. C. J. Donoghue, Dating tips for divergence-time estimation. *Trends Genet.* **31**, 637–650 (2015).

46. R. M. D. Beck, M. S. Y. Lee, Ancient dates or accelerated rates? Morphological clocks and the antiquity of placental mammals *Proc. Royal Soc. B* **281**, 20141278 (2014).

47. R. M. D. Beck, D. De Vries, M. C. Janiak, I. B. Goodhead, J. P. Boubli, Total evidence phylogeny of platyrrhine primates and a comparison of undated and tip-dating approaches. *J. Hum. Evol.* **174**, 103293 (2023).

48. S. Klopfstein, T. Spasojevic, Illustrating phylogenetic placement of fossils using RoguePlots: An example from ichneumonid parasitoid wasps (Hymenoptera, Ichneumonidae) and an extensive morphological matrix. *PLoS One* **14**, e0212942 (2019).

49. E. C. Kirk, E. L. Simons, Diets of fossil primates from the fayum depression of Egypt: A quantitative analysis of molar shearing. *J. Hum. Evol.* **40**, 203–229 (2001).

50. K. C. Beard, T. Qi, M. R. Dawson, B. Wang, C. Li, A diverse new primate fauna from middle Eocene fissure-fillings in southeastern China. *Nature* **368**, 604–609 (1994).

51. K. C. Beard, Y. Tong, M. R. Dawson, J. Wang, X. Huang, Earliest complete dentition of an anthropoid primate from the late middle Eocene of Shanxi Province, China. *Science* **272**, 82–85 (1996).

52. L. Marivaux *et al.*, Anthropoid primates from the Oligocene of Pakistan (Bugti Hills): Data on early anthropoid evolution and biogeography. *Proc. Natl. Acad. Sci. U.S.A.* **102**, 8436–8441 (2005).

53. K. C. Beard, Out of Asia: Anthropoid origins and the colonization of Africa. *Ann. Rev. Anthropol.* **45**, 199–213 (2016).

54. L. Marivaux, M. Boivin, Emergence of hystricognathous rodents (Mammalia, Hystricognathi): Palaeogene fossil record, phylogeny, macroevolution and historical biogeography. *Zool. J. Linn. Soc.* **187**, 929–964 (2019).

55. S. M. Bohaty, J. C. Zachos, F. Florondo, M. L. Delaney, Coupled greenhouse warming and deep-sea acidification in the middle Eocene. *Paleoceanography* **24**, PA2207 (2009).

56. R. P. Speijer, H. Pälike, C. J. Hollis, J. J. Hooker, J. G. Ogg, "The Paleogene period" in *Geological. Time Scale 2020* (Elsevier BV, 2020), pp. 1087–1140.

57. A. Mulch *et al.*, Rapid change in high-elevation precipitation patterns of Western North America during the Middle Eocene Climatic Optimum (MECO). *Am. J. Sci.* **315**, 317–336 (2015).

58. R. D'Onofrio *et al.*, Impact of the Middle Eocene Climatic Optimum (MECO) on foraminiferal and calcareous nannofossil assemblages in the Neo-Tethyan Baskil section (eastern Turkey): Paleoenvironmental and paleoclimatic reconstructions. *Appl. Sci.* **11**, 11339 (2021).

59. S. Peris Cabré *et al.*, Fluvio-deltaic record of increased sediment transport during the Middle Eocene Climatic Optimum (MECO), Southern Pyrenees, Spain. *EGUsphere*, in press (2022).

60. K. C. Beard, G. Métais, F. Ocakoğlu, A. Licht, An omomyid primate from the Pontide microcontinent of north-central Anatolia: Implications for sweepstakes dispersal of terrestrial mammals during the Eocene. *Geobios* **66–67**, 143–152 (2021).

61. R. F. Kay, "A new primate from the early Miocene of Gran Barranca, Chubut Province, Argentina: Paleoecological implications" in *The Paleontology of Gran Barranca: Evolution and Environmental Change through the Middle Cenozoic of Patagonia*, R. H. Madden, A. A. Carlini, M. G. Vucetich, R. F. Kay, Eds. (Cambridge University Press, 2010), pp. 216–235.

62. R. F. Kay, New World monkey origins. Fossils in Peru raise questions about the early evolution of monkeys in South America. *Science* **347**, 1068–1069 (2015).

63. R. F. Kay *et al.*, "Paleobiology of Santacrucian primates" in *Early Miocene Paleobiology in Patagonia: High-Latitude Paleocommunities of the Santa Cruz Formation*, S. F. Vizcaino, R. F. Kay, M. S. Bargo, Eds. (Cambridge University Press, 2012), pp. 306–330.

64. L. Marivaux, F. R. Negri, A. M. Ribeiro, 3D model related to the publication: An eosimiid primate of South Asian affinities in the Paleogene of Western Amazonia and the origin of New World monkeys. *MorphoMuseuM* **9**, e188 (2023), 10.18563/journal.m3.188.

65. R. J. Smith, Logarithmic transformation bias in allometry. *Am. J. Phys. Anthropol.* **90**, 215–228 (1993).

66. R. F. Kay, The evolution of molar occlusion in the Cercopithecidae and early catarrhines. *Am. J. Phys. Anthropol.* **46**, 327–352 (1977).

67. K. L. Allen, S. B. Cooke, L. A. Gonzales, R. F. Kay, Dietary inference from upper and lower molar morphology in platyrrhine primates. *PLoS One* **10**, e0118732 (2015).

68. M. S. Springer, E. Teeling, O. Madsen, M. J. Stanhope, W. W. De Jong, Integrated fossil and molecular data reconstruct bat echolocation. *Proc. Natl. Acad. Sci. U.S.A.* **98**, 6241–6246 (2001).

69. N. M. Jameson Kiesling, S. V. Yi, K. Xu, F. G. Sperone, D. E. Wildman, The tempo and mode of New World monkey evolution and biogeography in the context of phylogenomic analysis. *Mol. Phylogenet. Evol.* **82**, 386–399 (2015).

70. H. Schneider, I. Sampaio, The systematics and evolution of New World primates–A review. *Mol. Phylogenet. Evol.* **82**, 348–357 (2015).

71. C. G. Schrago, H. N. Seuánez, Large ancestral effective population size explains the difficult phylogenetic placement of owl monkeys. *Am. J. Primatol.* **81**, e22955 (2019).

72. L. E. Watrous, Q. D. Wheeler, The outgroup comparison method of character analysis. *Syst. Zool.* **30**, 1–11 (1981).

73. D. L. Swofford, PAUP*. Phylogenetic Analysis using Parsimony (*and Other Methods) (Version 4, Sinauer Associates, Sunderland, MA, 2002).

74. K. Bremer, The limits of amino acid sequence data in angiosperm phylogenetic reconstruction. *Evolution* **42**, 795–803 (1988).

75. F. Ronquist *et al.*, A total-evidence approach to dating with fossils, applied to the early radiation of the Hymenoptera. *Syst. Biol.* **61**, 973–999 (2012).

76. P. O. Lewis, A Likelihood approach to estimating phylogeny from discrete morphological character data. *Syst. Biol.* **50**, 913–925 (2001).

77. J. Barido-Sottani, D. Żyla, T. A. Heath, Estimating the age of poorly dated fossil specimens and deposits using total-evidence approach and the fossilized birth-death process. *Syst. Biol.*, 10.1093/sysbio/syac073 (2023).

78. F. Ronquist *et al.*, MrBayes 3.2: Efficient Bayesian phylogenetic inference and model choice across a large model space. *Syst. Biol.* **61**, 539–542 (2012).

79. M. A. Miller *et al.*, A RESTful API for access to phylogenetic tools via the CIPRES science gateway. *Evol. Bioinf.* **11**, 43–48 (2015).

80. R Development Core Team, *R: A Language and Environment for Statistical Computing* (Foundation for Statistical Computing, 2018).

81. E. Paradis, K. Schliep, ape 5.0: An environment for modern phylogenetics and evolutionary analyses in R. *Bioinformatics* **35**, 526–528 (2019).

82. D. W. Bapst, paleotree: An R package for paleontological and phylogenetic analyses of evolution. *Methods Ecol. Evol.* **3**, 803–807 (2012).